Insight into the Factors Influencing the Backbone Dynamics of Three Homologous Proteins, Dendrotoxins I and K, and BPTI: FTIR and Time-Resolved Fluorescence Investigations

Michelle Hollecker,*,‡ Michel Vincent,§ Jacques Gallay,§ Jean-Marie Ruysschaert,|| and Erik Goormaghtigh||

Centre de Biophysique Moléculaire, UPR 4301 CNRS, affiliée Université Orléans et INSERM, Rue Charles-Sadron, 45071 Orléans Cedex 2, France, LURE Bâtiment 209D, UMR 130 CNRS Université Paris-Sud, 91898 Orsay Cedex, France, and Laboratoire de Chimie Physique des Macromolécules aux Interfaces, Université Libre de Bruxelles, CP 206/2, Boulevard du Triomphe, B-1050 Bruxelles, Belgium

Received July 29, 2002

ABSTRACT: Attenuated total reflection Fourier transform infrared (ATR-FTIR) spectroscopy, combined with hydrogen/deuterium exchange technique and time-resolved fluorescence spectroscopy, has been used to investigate the changes in structure and dynamics that underlie the thermodynamic stability differences observed for three closely homologous proteins: dendrotoxins I and K, and bovine pancreatic trypsin inhibitor (BPTI). The experiments were performed on proteins under their native state and a modified form, obtained by selective reduction of a disulfide bond at the surface of the molecule, increasing slightly the backbone flexibility without changing the average structure. The data confirmed the high local as well as global rigidity of BPTI. In protein K, the exchange process was slow during the first 2 h of exchange, presumably reflecting a compact three-dimensional conformation, and then increased rapidly, the internal amide protons of the β-strands exchanging 10-fold faster than in BPTI or protein I. The most probable destabilizing element was identified as Pro32, in the core of the β-sheet. Protein I was found to present a 10% more expanded volume than protein K or BPTI, and there is a possible correlation between the resulting increased flexibility of the molecule and the lower thermodynamic stability observed for this protein. Interestingly, the interior amide protons of the β-sheet structure were found to be as protected against exchange in protein I as in BPTI, suggesting that, although globally more flexible than that of Toxin K or BPTI, the structure of Toxin I could be locally quite rigid. The structural factors suspected to be responsible for the differences in internal flexibility of the two toxins could play a significant role in determining their functional properties.

Dendrotoxins I and K are small globular proteins of about 60 amino acid residues, isolated from the venom of mamba snakes (*Dendroaspis polylepis polylepis*), that have been shown to specifically target neuronal voltage-sensitive potassium channels with high affinities (*1*). These two toxins are homologous to the Kunitz proteinase inhibitors (*2*, *3*) and have been shown by 2D-NMR as well as crystallographic studies to adopt nearly identical three-dimensional architectures as BPTI (bovine pancreatic trypsin inhibitor).[1] They are composed of one turn of a 3_{10}-helix at the N-terminus (5−7 residues), a 10-residue C-terminal α-helix, and a central two-stranded β-sheet (about 14 residues), with the two strands connected by a distorted β-turn of 4 residues (*4*−*8*). This folded structure is further stabilized by three disulfide bridges: Cys30−Cys51 and Cys5−Cys55 respectively connecting the β-sheet and the 3_{10}-helix to the α-helix, and Cys14−Cys38, linking the two flexible loops 11−16 and 37−42 (in this paper the residues are numbered according to BPTI). Interestingly, although structurally identical, the three homologues exhibit very different conformational stabilities, native protein K and protein I being, relative to their fully reduced forms with no disulfide bonds, respectively, 1.5 and 4.2 kcal/mol less stable than native BPTI (*9*).

The pattern of folding of BPTI, Toxin K, and Toxin I are also closely related (*9*). The three homologues fold via the same primary intermediates (named after the disulfide bonds they contain), and the folding kinetics are consistent with the same pathways being followed. Yet there is no clear correlation between the rates of refolding and the global thermodynamic stabilities of the final folded states, as protein K refolds faster than its two homologues (*9*). In an attempt to better understand the conformational factors that direct the folding and determine the backbone dynamics and the function of this family of proteins, we have undertaken a comparative study of the kinetics of amide proton exchange of the three homologues, using Fourier transform infrared spectroscopy. The experiments were performed on native

* Corresponding author. E-mail: holleck@cnrs-orleans.fr.
‡ Centre de Biophysique Moléculaire.
§ LURE, Université Paris-Sud.
|| Université Libre de Bruxelles.

[1] Abbreviations: BPTI, Bovine pancreatic trypsin inhibitor; ATR-FTIR, attenuated total reflection Fourier transform infrared; NMR, nuclear magnetic resonance; PIPES, piperazine-*N*,*N*′-bis(2-ethane) sulfonic acid; CM1,2-protein, native protein with the 14−38 disulfide bond reduced and the resulting thiols protected by carboxymethylation; CD, circular dichroism; MEM, maximum entropy method; NLLSQ, nonlinear least squares; amide I′, amide I after deuteration.

10.1021/bi0204950 CCC: $22.00
Published on Web 11/26/2002

BPTI, protein K, and protein I and on a modified form of these proteins, obtained by selective reduction of the disulfide bond between cysteine 14 and cysteine 38 (also noted cystine 14−38), followed by carboxymethylation of the cysteinyl residues. Disulfide 14−38 being mainly solvent-exposed, its reduction has been shown by NMR for BPTI (*10*) and by CD spectroscopy for Toxins K and I (*11*) to induce only very local changes in the conformation of the three proteins. However, a strong effect on the thermodynamic stability and internal flexibility of the molecule has been reported in the case of BPTI (*10*) and should be expected for the two toxins. To interpret our infrared results on BPTI, native and modified (noted CM1,2-BPTI), we relied mainly on the very thorough NMR work done on these proteins by Wüthrich and co-workers (*10*, *12*, *13*). The 2D-NMR solution structures of native Toxins I and K were also available in the literature (*4*−*8*), but very little conformational investigation had been done on the modified forms CM1,2-I and CM1,2-K, apart from the circular dichroism study cited above (*11*); in particular, there was a lack of information on the extent of local conformational changes, albeit small, induced by the reduction of disulfide bond 14−38 and the introduction of two charged blocking groups in this flexible part of the molecule, that we compensated partly by performing time-resolved fluorescence spectroscopy measurements on the four dendrotoxin species, using the fluorescence properties of the single tryptophanyl residue they contained.

EXPERIMENTAL PROCEDURES

Protein Samples. BPTI (Aprotinin) was purchased from Boehringer, Mannheim. Desiccated crude venom of *Dendroaspis polylepis polylepis* was obtained from Jonathan Leakey Ltd, East Africa. Dendrotoxins I and K were extracted from the crude venom by gel filtration on Sephadex G50, followed by two successive separations by cation-exchange chromatography as described previously (*9*). The selective reduction of disulfide bond 14−38 was performed at room temperature, in 0.1 M Tris-Hcl (pH 8.7), 0.2 M Kcl, 1 mM EDTA, and 2.5 mM reduced dithiothreitol for 1−2 min. The reaction was then quenched by the addition of potassium iodoacetate to a final concentration of 0.1 M and the modified protein species further purified on a CM52 column (*9*). The purity of all samples was checked by electrospray mass spectrometry.

For all the experiments described in this paper, the proteins were dissolved in 6 mM Pipes/NaOH, pH 6.8, to a concentration of 5 mg/mL for the infrared measurements, 1 mg/mL in the case of the fluorescence experiments.

Preparation of Fully Deuterated Samples. To obtain the fully deuterated protein samples, 2 mg of protein was dissolved in ^2H_2O and incubated overnight at 65°. The next day, the samples were lyophilized and then dissolved in 6 mM Pipes buffer in ^2H_2O (p^{2}H 6.8), and the infrared spectra were recorded.

Infrared Measurements. Attenuated total reflection infrared (ATR-FTIR) spectra were recorded at room temperature on a Perkin-Elmer infrared spectrophotometer 1720X equipped with a liquid nitrogen cooled MCT detector. The spectrophotometer was continuously purged with dry air. The internal reflection element was a germanium ATR plate (50 × 20 × 2 mm) with an aperture angle of 45°. Thin films were obtained by spreading and slowly evaporating 20 μL of protein stock solution (to a total of 100 μg) on one side of a germanium plate (50 × 20 × 2 mm, Harrick, Ossining, NY) under a N_2 stream (*14*). Under these conditions, the water contribution was found negligible in the amide I area of the spectra (data not shown). The plate was then sealed in a universal sample holder containing a gas in-let and an out-let, allowing the sample to be exposed to any controlled atmospheric condition. Nitrogen gas was saturated with ^2H_2O by flushing it through a series of five vials containing 1−2 mL of ^2H_2O, at a flow rate of 50 mL/min (controlled by a Brooks flow meter). Bubbling was started at least 1 h before starting the experiment. At the zero time, the tubing was connected to the cavity of the sealed chamber surrounding the film.

Hydrogen/Deuterium Exchange. All the species were stable over the time of the experiment. Before starting the deuteration, 10 spectra of each sample were recorded in order to test the reproducibility of both the measurements and the area determination; their averaged spectrum was used as the 0% deuteration of the kinetics curves. For each kinetic time point, 12 spectra were recorded between 1400 and 1800 cm^{-1} and averaged at a resolution of 4 cm^{-1}. At the end of the scan, the spectra were automatically transferred from the memory of the spectrophotometer to a computer for subsequent treatments. At the beginning of the kinetics, spectra were recorded every 15 s. After the first 2 min, the time interval was exponentially increased up to a total of 10−13 h of exposure. After the first 16 min, the interval between the scans was large enough to allow the interdigitation of a second kinetic. A second sample placed on another ATR setup of the Perkin-Elmer sample shuttle was then analyzed with the same sampling but with a 16 min offset by connecting the ^2H_2O-saturated N_2 flow in series with the first sample. From this time on, the program changed the shuttle position to follow both kinetics. All the kinetic curves presented in the results and discussion section are the averages of two to three separate hydrogen exchange kinetic experiments.

Analysis of Infrared Spectra. The residual water vapor contribution was automatically subtracted from the spectra; the subtraction coefficient was computed as the ratio of the area of the atmospheric water band integrated between 1565 and 1551 cm^{-1} on the protein sample spectrum and on the corresponding background spectrum. When mentioned, spectra were deconvoluted using a Lorentzian line shape with a line width at half-height of 19 cm^{-1}, followed by a Gaussian apodization with a line width at half-height of 11 cm^{-1}, yielding to a resolution enhancement factor of 1.6. The area of amides I, I′, and II were obtained by automatic integration. For each spectrum, the area of amide II was divided by the area of amide I in order to take into account the swelling of the sample layer due to the presence of ^2H_2O (*15*).

All kinetic curves were analyzed as multiexponential decays of populations α_i of amide protons with the same rate-constants k_i, using a nonlinear-least-squares procedure (NLLSQ). Starting with the exchange data obtained for native BPTI, a minimum of five to six exponential terms were needed for the analysis to converge and a satisfactory fitting of the kinetic curve be obtained. The analysis was performed in three successive steps: (i) fixing approximately the

number of protons with exchanging times higher than 2 h, to determine the rate constants of fast exchanging protons, (ii) fixing the rate constants for fast exchanging protons using the values obtained in step i and replacing the previous constraint with one to two exponential functions to describe the exchange at longer times, and (iii) performing a last NLLSQ analysis on the values obtained in steps i and ii in order to determine the entire set of rate constant values. We obtained rate constants ranging from 4 to 10^{-4} min^{-1}, which were in very good accordance with the values already published in the literature for the amide-proton exchange of BPTI (*16*), using NMR and infrared techniques. The kinetic curves of protein K and protein I were analyzed in the same way, by taking the set of values (k_i, α_i) obtained for native BPTI as initial parameters and performing a NLLSQ analysis to fit the experimental curves. In turn, the kinetic curves of the three CM1,2-modified species were analyzed with the set of values (k_i, α_i) previously obtained for the corresponding native protein, as initial parameters.

Time-Resolved Fluorescence Measurements. Fluorescence intensity and anisotropy decays were obtained by the time-correlated single photon counting technique from the polarized components $I_{vv}(t)$ and $I_{vh}(t)$ on the experimental setup installed on the SB1 window of the synchrotron radiation machine Super-ACO (Anneau de Collision d'Orsay) (*17*). The excitation and the emission wavelengths were selected, respectively, by a double monochromator (Jobin Yvon UV-DH10, bandwidth 4 nm) and by a single monochromator (Jobin Yvon UV-H10, bandwidth 10 nm). A MCP-PMT Hamamatsu detector (model R3809U-02) was used. Time resolution was ~20 ps, and the data were stored in 2048 channels. Automatic sampling cycles including 30 s accumulation time for the instrument response function and 90 s acquisition time for each polarized component were carried out until a total number of $2-4 \times 10^6$ counts was reached in the fluorescence intensity decay.

Data Analysis of Fluorescence Intensity and Anisotropy Decays. Analysis of fluorescence intensity decays as sums of exponential terms was performed by the maximum entropy method (MEM) (*17, 18*).

The one-dimensional model of the anisotropy, in which each lifetime is coupled to any rotational correlation time (*19*), systematically performed analyses of the polarized fluorescence decays. Sets of 150 and 100 independent variables, equally spaced in log scale, were used for the fluorescence intensity and anisotropy decays, respectively.

A two-dimensional (τ,θ) analysis, essential to describe the coupling between lifetimes and rotational correlation times, was also used (*20, 21*). This analysis starts with an initial model of the (τ,θ) distribution as a "flat" map where all the (τ,θ) are equiprobable. It allows the delineation of the (τ,θ) associations with the less possible a priori hypotheses. The two-dimensional analyses were carried out on a DEC alpha computer Vax 7620 with a set of 1600 independent variables (40 τ and 40 θ equally spaced in log scale). The programs including the MEMSYS 5 subroutines (MEDC Ltd., Cambridge, U.K.) were written in double precision FORTRAN 77.

RESULTS AND DISCUSSION

FTIR Spectra and Kinetics of Deuterium Exchange. Infrared spectroscopy is a powerful technique for studying protein structure and dynamics and is particularly sensitive to small changes in protein conformation. The information obtained by this method are complementary: the amide I band (1700−1600 cm^{-1}) generally shifts by 5−10 cm^{-1} to lower wavenumber (amide I′) upon hydrogen exchange and is characteristic of the secondary structure of a protein (*22*), whereas the changes in intensity of the amide II (1600−1500 cm^{-1}) or amide II′ (1500−1400 cm^{-1}) regions (Figure 1) during deuteration reflect the exchange of the backbone amide-protons and, hence, the flexibility of the molecule (*15*).

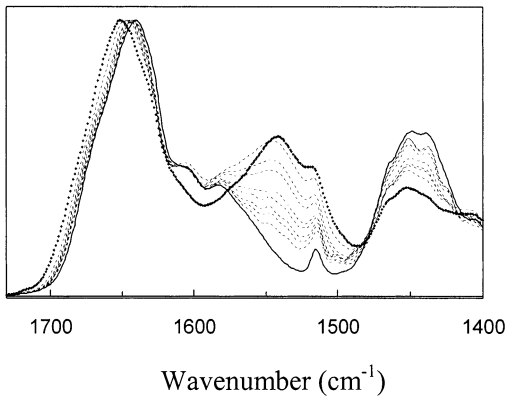

FIGURE 1: IR spectra of native protein K in (• •) H_2O, (—) D_2O, and (---) at different times of exchange ranging between 0.5 and 640 min and showing the amide I (1700−1600 cm^{-1}), the amide II (1600−1500 cm^{-1}), and the amide II′ (1500−1400 cm^{-1}) regions.

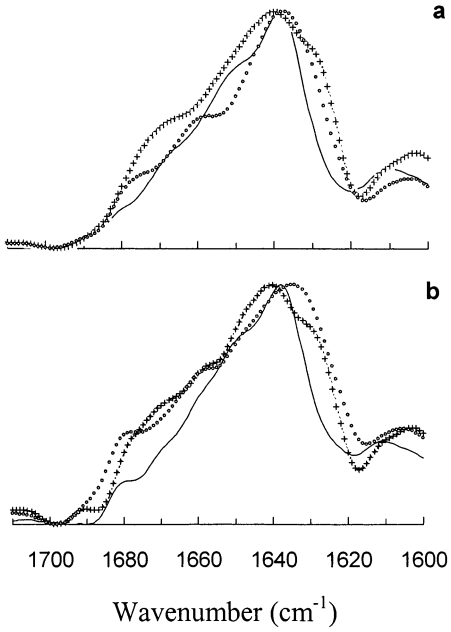

FIGURE 2: IR spectra in the amide I region of a film of (a) native and (b) modified proteins: (—) BPTI, (+) Toxin K, (○) Toxin I, after deconvolution using a Lorentzian line shape with 19 cm^{-1} full width at half-height, followed by a Gaussian apodization with a line width at half-height of 11 cm^{-1}.

Comparisons of the deconvoluted amide I′ regions of the native proteins and their modified forms are presented in Figure 2a,b. To follow the kinetics of deuterium exchange, the intensity of amide II normalized to amide I was plotted as a function of time of exchange for the different species (Figures 3 and 4), and the kinetic curves were analyzed as described in the experimental procedures section. There was a remarkable correlation between the series of rate constants

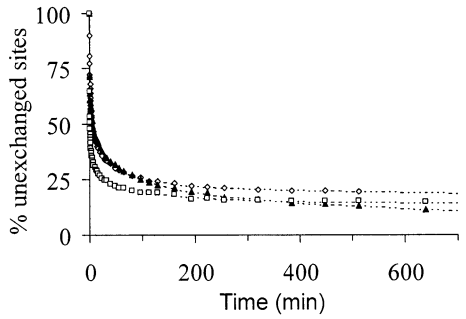

FIGURE 3: Kinetics of exchange of the native proteins, BPTI (◇), Toxin K (▲), and Toxin I (□). The kinetics were obtained by plotting the amide II/amide I ratio as a function of time exposure of a film of protein to ^2H_2O.

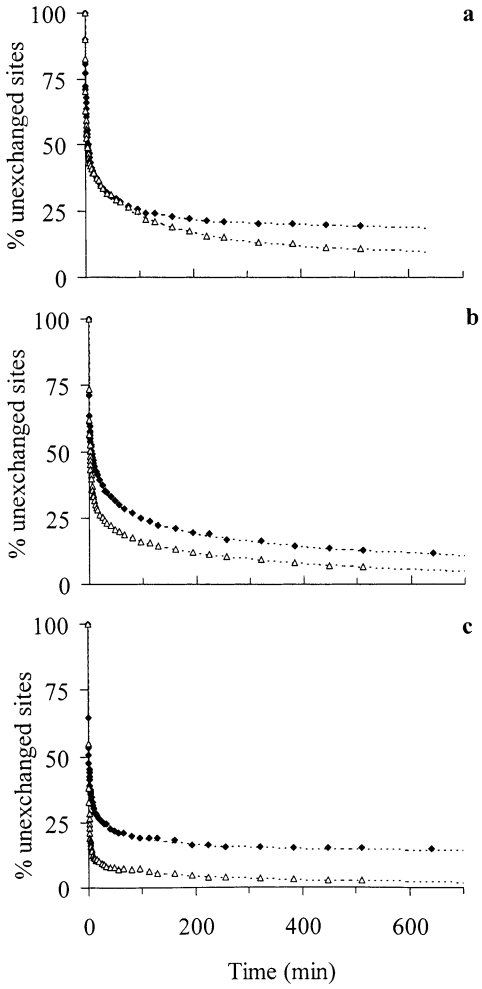

FIGURE 4: Kinetics of exchange of the native (◆) and modified (△) proteins: (a) BPTI, (b) Toxin K, and (c) Toxin I. The kinetics were obtained by plotting the amide II/amide I ratio as a function of time exposure of a film of protein to ^2H_2O.

obtained for the different species, and each curve could be adequately described by a set of five to six populations with decay times ranging from 0.2 min to over 5 days; the fits of the curves obtained are shown by the dashed lines in Figures 3 and 4, and the populations and exchange rates of these fits are reported in Table 1. The exchange rates we obtained by ATR-FTIR for native BPTI were in close agreement with those reported by NMR spectroscopy (*13*, *23*), after taking into account the different experimental conditions of p^{2}H and temperature used in the two techniques (*16*).

In a previous NMR investigation on a variety of BPTI chemically modified forms (*24*−*26*), it was demonstrated that, provided the spatial structure of BPTI is preserved in a species, the rank order of the exchange rates for individual amide protons is the same than in native BPTI. As this applies to the homologous proteins under study (*4*−*8*), we took this NMR work as a guideline. Knowing, from their NMR structure, the number of residues that participate in the different secondary structure elements of the three proteins, we tentatively assigned the groups of most slowly exchanging protons observed in the kinetics of exchange of the different species to the central region of the β-sheet, the amide protons at the two ends of the β-sheet being assumed to exchange faster but not as fast as the hydrogen-bonded amide protons of the α-helix. The protons exchanging with a decay time of 2−3 min were attributed to the β-turn region, the 3_{10}-helix, and those backbone protons not belonging to a secondary structure, but protected from exchange by the rest of the molecule. All the protons readily exchanged within less than 0.5 min after the beginning of the experiment were considered to belong to unordered regions and/or in close contact with the solvent (Table 1). Considering all amide protons with rate constants inferior to 10^{-1} min^{-1} as slowly exchanging (corresponding to rate constants inferior to 10^{-4} obtained by NMR at p^{2}H 3.5), we obtained, by the IR approach, numbers of slowly exchanging protons of 32 in native BPTI, 30 in protein K and 22 in protein I, that were in very good correlation with the corresponding NMR values reported in the literature of 33 in BPTI (*13*, *23*), 29 in protein K (*4*) and 22 in protein I (*7*).

The High Rigidity of BPTI Tertiary and Secondary Structures Is Confirmed. The amide I′ band of BPTI displayed a maximum around 1638 cm^{-1} and shoulders at 1649, 1666, and 1680 cm^{-1} (Figure 2a) that are usually assigned to unordered, α-helix, β-turn and/or 3_{10}-helix, and β-turn and β-sheet, respectively (*27*, *28*). The observed kinetics of exchange for protein K and BPTI showed only minor differences during the first hour of exchange (Figure 3 and Table 1). Around 6 amide backbone protons belonging to unordered structures were better protected in native BPTI than in protein K, but exchanged within 0.5 min in the modified form CM1,2-BPTI. When disulfide bond 14−38 is reduced, a narrow cleft between the two flexible loops 11−16 and 37−42 is created, where water can penetrate (*13*). The impact of such a modification on the average spatial structure of BPTI is reported to be very small, mainly affecting the peptide backbone fragments 35−40, while other molecular regions remain nearly unchanged (*10*); therefore, the unordered residues not readily exchanged in native BPTI most probably correspond to those backbone protons belonging to the two loops connected by the bond 14−38, as they are directly affected by the modification.

The reduction of disulfide bond 14−38 in BPTI had only a small effect on the exchange of the amide protons belonging to the α-helix (Table 1 and Figure 4a), but it affected more strongly the stability against exchange of part of the protons assigned to the central β-strands, 10 of them having their decay time of exchange reduced from over 5 days to less than 16 h. Nevertheless, a core of ∼2 highly protected amide protons still existed, attesting to the high rigidity of the β-sheet in the BPTI structure.

Table 1: Kinetic Parameters for the Amide-Proton Exchange Monitored at p^{2}H 6.8 and 20 °C by FTIR Spectroscopy

N-BPTI			N−K			N−I		
Sec. Structure[a]	N[b]	k (min^{-1})	Sec. Structure	N	k (min^{-1})	Sec. Structure	N	k (min^{-1})
un.	13.6	4.55	un.	19.8	6.04	un. + 3_{10}	30.0	5.00
t.(4) + un.	12.8	4.37×10^{-1}	3_{10}(1) + t.(4) + un.	7.0	5.42×10^{-1}	α-h(3) + t.	8.3	4.26×10^{-1}
3_{10}(7) + α-h	8.4	9.69×10^{-2}	3_{10}(6) + α-h	6.9	6.87×10^{-2}	α-h	7.0	6.15×10^{-2}
α-h(9) + β-sh	9.6	1.64×10^{-2}	α-h.(9)	9.1	1.51×10^{-2}	β-sh	5.3	8.61×10^{-3}
β-sh	1.9	3.30×10^{-3}	β-core + β-sh	8.9	2.54×10^{-3}	−	−	−
β-core	11.6	1.25×10^{-4}	β-core	5.2	1.25×10^{-4}	β-core	9.3	1.25×10^{-4}
CM1, 2BPTI			CM1, 2-K			CM1,2-I		
Sec. Structure	N	k (min^{-1})	Sec. Structure	N	k (min^{-1})	Sec. Structure	N	k (min^{-1})
un. + t.(1)	23.6	2.29	un.	20.39	4.02	un. + 3_{10} + t.	36.1	4.71
3_{10}(5) + t.	7.9	2.39×10^{-1}	3_{10}(7) + t.(4) + un.	12.82	6.49×10^{-1}	α-h(10) + β-sh	13.8	6.64×10^{-1}
α-h(1) + 3_{10}	3.2	6.67×10^{-2}	α-h	7.09	1.04×10^{-1}	β-sh	4.5	1.01×10^{-1}
α-h(9) + β-sh	13.9	9.81×10^{-3}	β-sh(3) + α-h	6.14	2.01×10^{-2}	β-core	3.3	6.98×10^{-3}
β-core	7.6	1.00×10^{-3}	β-core	8.4	3.03×10^{-3}	β-core	2.4	1.00×10^{-3}
β-core	1.6	1.25×10^{-4}	β-core	2.12	1.25×10^{-4}	−	0.0	1.25×10^{-4}

[a] Abbreviations used for the secondary structure elements: un., unordered; t., β-turn; 3_{10}, 3_{10}-helix; α-h, α-helix; β-sh., β-sheet (in brackets is an estimate of the numbers of amino acid residues that participate to the corresponding secondary structure). [b] Calculated number of residues with a rate constant k.

Protein K Is a Compact Molecule with a Destabilized β-Sheet. Compared to BPTI and protein I (Figure 2a), the infrared spectrum of native protein K was broader and characterized by a marked shift to longer wavenumbers of the band attributed to unordered structure, indicative of some structural differences in the two loops region for the three proteins. BPTI contains four internal water molecules; one of them is located in the loops region and forms hydrogen bonds with residues Thr11, Cys14, and Cys38 (*23*). Due to amino acid substitutions, this water molecule has been displaced in the case of the two toxins, and the NMR 3-D structure of protein K indicates a difference, compared to BPTI, for the tripeptide 39−40−41, that was explained by the need of proper positioning of Asn41, to match the geometry of the missing water molecule (*6*). The observed shift of the maximum, in the infrared amide I′ spectrum of protein K, compared to BPTI, could be an effect of the resulting compaction in the loops region. Such a displacement was not reported in the case of protein I (*7*, *8*).

The major difference between the kinetics of exchange of native BPTI and protein K was observed for the most slowly exchanging residues attributed to the central region of the β-sheet (Figure 3 and Table 1). In BPTI, 11 of these residues formed a very rigid β-core, with a decay time of exchange superior to 5 days; in protein K, such a core of residues exchanging more slowly than all the others also existed, but only five of them had a decay time superior to 5 days, the rest exchanging within a few hours. As the peripheral part of the β-strands, as well as the α-helix and part of the 3_{10}-helix, were found to exchange slightly more slowly in native protein K than in BPTI, the strong loss of stability against exchange observed for the central part of the β-strands appears to be correlated not as much with a global higher flexibility of the molecule than with a strong destabilizing element within the β-core of protein K structure. Consistent with this interpretation, the amide I′ region of the infrared spectra (Figure 2a,b) of protein K showed two bands at 1630 and 1667 cm^{-1} that were unusually strong, suggesting the existence of a conformational perturbation in the β-sheet/β-turn region (*27*, *29*).

In contrast to BPTI, protein K contains two prolyl residues within the β-sheet: Pro19, at a peripheral position, and Pro32, in the central part of the strands. Prolyl residues are not usually found in standard β-sheet structures (*30*), and displacements of large segments of the polypeptide chain, due to the introduction of Pro32 residue within the β-sheet, as well as differences in the backbone conformation of the β-turn, have been reported for protein K (*6*). Spatially, residue 32 is in a region of the molecule containing hydrophobic clusters that have been previously described as "pillars for the architecture of the protein molecule" (*25*), and the introduction of a prolyl residue in the immediate vicinity of these clusters appears as the most probable cause for the drastic loss of stability against exchange observed in the corresponding region.

Reduction of Disulfide Bond 14−38 is Less Destabilizing for Protein K than for BPTI. The kinetic of exchange of protein K was only slightly affected by the reduction of cystine 14−38; in particular, the number of amide protons in direct contact with the solvent was not increased, as would have been expected after opening of a cleft in the structure (Table 1). A general reduction of the half-lives of the amide protons belonging to the helices was observed, but the exchange rates of the core of buried residues in the β-strands were less affected by the conformational modification than in the corresponding BPTI species.

Protein K has a single tryptophanyl residue located at position 25, in the β-turn region between the two strands of the β-sheet, and at the opposite end of the molecule from disulfide bond 14−38. This fluorophore is mainly solvent-exposed, as confirmed by the emission λ_{max} value near 350 nm for both native and modified proteins (Table 2); yet probably because of its packing requirements, as well as of the immediate proximity in the β-turn of Lys24, Lys26 and Lys28, it was reported to have very little independent motion (*6*). Therefore, although far from the modification site, Trp25 should be a good reporter of any global conformational change occurring in protein K after reduction of disulfide bond 14−38.

Table 2: Trp Fluorescence Emission Maximum and Time-Resolved Intensity Parameters of Toxins I and K[a]

protein[b]	λ_{max} (nm)	τ_1 (ns) (α_1)	τ_2 (ns) (α_2)	τ_3 (ns) (α_3)	$\langle t \rangle$ (ns)[c]
N−K	350.0	0.41 (0.26)	1.57 (0.73)	5.40 (0.01)	1.17
CM1,2-K	350.0	0.37 (0.32)	1.48 (0.65)	3.33 (0.03)	1.18
N−I	338.5	0.70 (0.07)	1.90 (0.93)	5.77 (0.01)	1.84
CM1,2-I	339.5	0.39 (0.06)	1.43 (0.20)	4.38 (0.74)	3.55

[a] MEM analysis was performed on the fluorescence intensity $S(t)$ reconstructed from the parallel and perpendicular polarized components $I_{vv}(t)$ and $I_{vh}(t)$ such as $S(t) = I_{vv}(t) + 2GI_{vh}(t) = \int_0^\infty a(\tau)e^{-t/\tau}\,d\tau$, where τ is the excited-state lifetime and $\alpha(\tau)$ its normalized amplitude. G is a correction factor accounting for the difference in transmission of the $I_{vv}(t)$ and $I_{vh}(t)$ components. τ_i and α_i are the values of the center and of the integrated normalized amplitudes of each lifetime peak, respectively. [b] The experiments were carried out at 20 °C and pH 6.8. For the time-resolved experiments, the excitation wavelength was 300 nm (bandwidth 4 nm), and the emission wavelength was 350 nm (bandwidth 10 nm). [c] The average lifetime was calculated using the equation $\langle \tau \rangle = \sum_{i=1}^{3} \alpha_i \tau_i$.

Table 3: Trp Fluorescence Anisotropy Decay Parameters of Toxins I and K, Obtained Using the One-Dimensional Analysis: $A(t) = [I_{vv}(t) - GI_{vh}(t)]/[I_{vv}(t) + 2GI_{vh}(t)] = \int_0^\infty \beta(\theta)e^{-t/\theta}\,d\theta$, where θ Is the Rotational Correlation Time and $\beta(\theta)$ Its Associated Anisotropy[a]

protein[b]	θ_1 (ns) (β_1)	θ_2 (ns) (β_2)	r_0[c]	R (Å)[d] (exp)	R (Å)[e] (calc)	ω_{max}[f] (deg)
N−K	0.05 (0.062)	3.1 (0.206)	0.268	14.8	14.2	26
CM1,2-K	0.05 (0.079)	2.9 (0.206)	0.285	14.3	14.3	26
N−I	−	4.4 (0.267)	0.267	16.1	14.6	0
CM1,2-I	0.25 (0.006)	4.2 (0.268)	0.274	15.9	14.6	11

[a] θ_i and β_i are the values of the center and of the integrated anisotropy value of each rotational correlation time peak, respectively. G has the same meaning as in the legend of the Table 2. [b] Excitation wavelength, 300 nm (bandwidth 4 nm); emission wavelength, 350 nm (bandwidth 10 nm). [c] The intrinsic anisotropy was calculated using the relation $r_0 = \sum_{i=1}^{2} \beta_i$. [d] The Stokes radius of the protein was calculated from the slope of θ_2 vs η/T using the relationship: $\theta_2 = (4/3\pi R^3)\eta/kT$, where η is the viscosity, k the Boltzman constant, and T the absolute temperature. [e] This theoretical radius was calculated from the amino acid composition of the protein assuming a partial specific volume of 0.73 mL/g and an additional hydration volume of 50% to account for the solvent shell. [f] The semiangle of the wobbling cone was calculated using the relation: $\beta_2/r_0 = [1/2(\cos \omega_{max})(1 + \cos \omega_{max})]^2$.

The fluorescence anisotropy decay measurements of Trp25 gave a biexponential decay with a major correlation time θ_2, usually associated with the Brownian motion of the molecule, in the range of 2.9−3.2 ns (Table 3). Assuming that the molecules are spherical in shape, θ_2 is related to the hydrodynamic volume V_h of the protein by the Stokes−Einstein relationship (see legend of Table 3). The dependence of θ_2 with the viscosity/temperature ratio was linear for both protein K species (regression coefficient values of 0.999), confirming the validity of the nearly spherical model. The slopes of these two curves, proportional to V_h, were, however, clearly distinct by ∼10% (not shown). The corresponding hydrodynamic radii values are presented in Table 3. One would expect CM1,2-K to present a slightly more expanded volume, due to the increased flexibility of the structure after reduction and introduction of two blocking groups; yet the measured hydrodynamic volume of this species was found to be 10% smaller than that in native protein K. Combined with the infrared data, these results suggest that, although the flexibility of the molecule should be increased at the modification site by the reduction of S−S bond 14−38, the two loops most probably stay in closer contact in CM1,2-K than in the native conformation, protecting better the interior amide protons against exchange than in the case of CM1,2-BPTI.

The Electrostatic Interactions Could Be More Stabilizing in CM1,2-K than in CM1,2-BPTI. Two factors can affect the local conformation at the modification site upon cleavage of cystine 14−38. The first one is an added flexibility of the two loops that were connected by that bond; the second one is the introduction of two charged blocking groups on the cysteinyl residues. Depending on their charges and the electrostatic distribution of charges in their vicinity, these two blocking groups can create either a repulsive effect, that will further destabilize the structure, or an attractive effect that should result in a partial closure of the cleft. In the present case, the residues Cys14 and Cys38 were protected with iodoacetate, introducing two negative side chains at the surface of the molecule. In BPTI, a stabilizing effect was reported, which was explained by short-range stabilizing interactions between the positively charged side chains of Lys15, Arg17, Arg20, Arg39, and Lys41 and the negatively charged groups introduced (*10*). While in BPTI the positively charged side chains are distributed throughout the modification site, in protein K there is a concentration of positive charges (Lys15, Arg16, and Lys17) on one of the loops, two negatively charged side chains, i.e., the blocking group on cysteinyl 38 and Asp34 being located on the other loop. Such a distribution of charges appears to be very favorable for the formation of a network of local stabilizing electrostatic interactions, as the exchange of the core residues was less affected by the modification in CM1,2-K than in CM1,2-BPTI. The decrease in volume observed in the case of CM1,2-K could be due to the disappearance of the steric hindrance of disulfide bond 14−38 in native protein K after reduction.

The Overall Structure of Protein I Is More Expanded and Flexible. The deconvoluted IR spectrum of protein I in D_2O was characterized by a maximum around 1638 cm^{-1} and two shoulders at 1659 and 1677 cm^{-1}, shifted from those observed in BPTI spectrum (Figure 2a). The kinetic of exchange of protein I was very fast, with 76% of the backbone amide protons exchanged within 0.5 h, confirming the higher flexibility of the folded structure.

Although the molecular architecture of protein I is essentially identical to those of BPTI and protein K (*7*, *8*), it presents local differences that could partly explain the global loss of rigidity observed for this protein. The structures of BPTI and protein K are stabilized by a salt bridge between the amino and the carboxyl termini, and the side chains of the corresponding residues are reported to be among the best defined ones in the structures of both proteins in solution (*31*). This bond, by keeping the α- and 3_{10}-helices in close contact to the rest of the molecule, contributes to the stability of the entire conformation against exchange. In protein I, the salt bridge between the N- and C-caps does not exist, and a difference in orientation of the 3_{10}-helix was reported, leaving part of the α-helix and β-sheet less shielded from the solvent (*8*). As a result, the 3_{10}- and α-helices amide protons were seen to exchange faster (Table 1). Nevertheless,

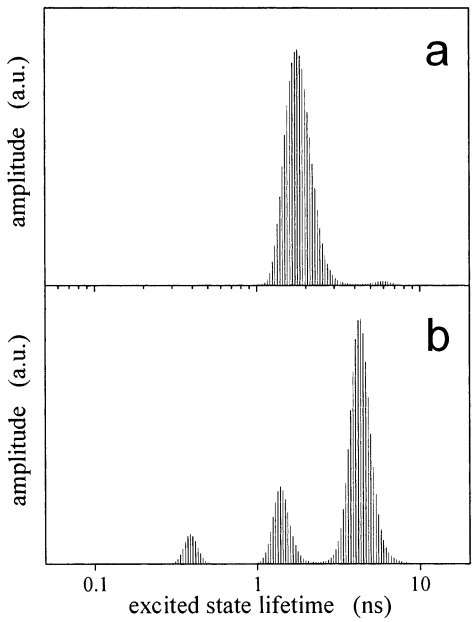

FIGURE 5: The excited-state lifetime profiles of native (a) and modified (b) Toxin I.

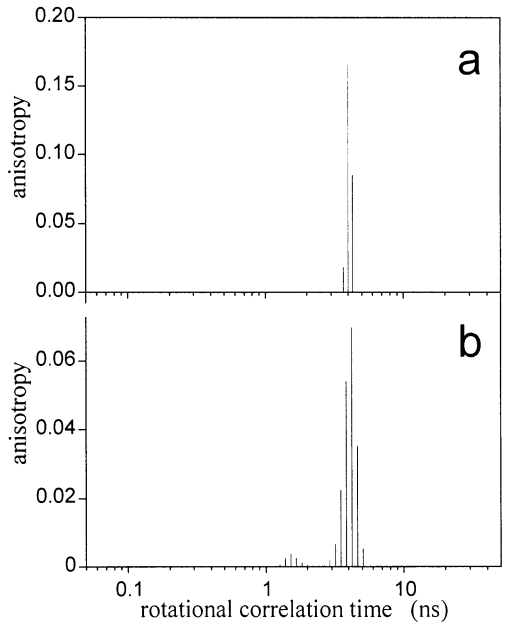

FIGURE 6: One-dimensional rotational correlation time distributions of native (a) and modified (b) Toxin I.

it should be noted that these secondary structure elements were clearly not disordered, as the amide I′ spectra showed the fine structure corresponding to them (Figure 2a).

At the opposite end of the molecule from the N- and C-terminals, the disulfide bridge 14−38 contributes to the thermodynamic stability of the folded structure by connecting the two flexible loops: Pro11-Lys16 and Gly37-Ser42. It is largely exposed on the surface of the folded protein and the last disulfide to form during the refolding of the three homologues, as well as the first to break during the unfolding process (*9*). The formation of disulfide bridge 14−38 in protein I was shown to be, respectively, 2 and 4 times slower than in Toxin K and BPTI, whereas its selective reduction was 1.3 times faster than in the two homologues (*9*); these are strong indications that the two loops region might also be more flexible in Toxin I than in BPTI or Toxin K. The broadening of the band attributed to unordered structure, observed in the deconvoluted amide I′ IR spectrum of native protein I, compared to BPTI (Figure 2a), further supports this conclusion.

Toxin I has a single tryptophan residue, Trp35, located in the region of the molecule containing the two flexible loops. The presence of Trp35 in the vicinity of cystine 14−38 is particularly advantageous as its fluorescence properties should report on any conformational changes induced in its environment upon reduction of this disulfide bond and be of help to correlate any loss of stability against exchange observed in CM1,2-I with specific structural features.

The fluorescence emission maximum of Trp35 in native protein I was 338.5 nm, suggesting that the indole ring was not completely buried within the molecule. Yet the fluorescence decay was almost monoexponential, with a major lifetime around 1.9 ns accounting for 93% of the total fluorescence intensity. Two very minor components could also be observable at 0.7 and 5.77 ns (Table 2 and Figure 5a). The major component had a lifetime unusually short for a tryptophanyl residue partly buried in a protein, which could be an effect of the proximity of cystine 14−38 (*32*) as, spatially, Trp35 is separated by only 7 Å from the disulfide bond 14−38 (*7*).

In native protein I, Trp35 was found to depolarize only by overall rotation of the protein matrix (Figure 6a), with a motional correlation time around 4.1−4.4 ns (Table 3). To assess the degree of exposure of the tryptophan residues in the different conformations, we performed collisional quenching measurements using increasing amounts of acrylamide as quencher. The average degree of exposure of a Trp residue is revealed by the magnitude of the bimolecular rate constant k_q, usually described as the frequency at which acrylamide encounters the fluorophore (*33*). The value of the bimolecular quenching rate constant k_q was derived from the slope of the Stern−Volmer plot, taking into account the average fluorescence lifetime (Table 3). We found a bimolecular quenching rate constant of 1.5×10^9 M^{-1} s^{-1} for Trp35 in native protein I. Compared to the k_q value of 3.5×10^9 M^{-1} s^{-1} given for a fully solvent exposed tryptophan residue rigidly attached to a protein (*34*, *35*), the solvent accessibility of Trp35 in the native structure obtained from the fluorescence data was 43%. As a comparison, the accessibility of Trp25 in protein K and its modified form was 57%.

In accord with a globally less compact conformation, the molecule of protein I presented a more expanded hydrodynamic volume than its two homologues, and the fluorescence anisotropy decay measurements gave an experimental hydrodynamic radius of 16.1 Å, instead of the calculated one of 14.6 Å (Table 3).

Although Less Shielded from the Solvent, the Amide Protons of the β-Sheet Are as Protected in Protein I as in BPTI. As a result of the globally more open structure of protein I, the kinetic of proton exchange showed a high number of NH groups that exchanged within less than 1 min and could correspond to the amide protons of the unordered structure and of the 3_{10}-helix, as they are in direct contact with the solvent. The amide protons of the α-helix and the β-turn were also less protected against exchange than in BPTI and protein K (Table 1 and Figure 3). Surprisingly, the

peripheral part, as well as the central part of the β-sheet, appeared quite well protected against exchange, and a core of nine deeply buried amide protons, usually attributed to the central β-strands, that was as stable in protein I as in BPTI could be observed.

In β-sheets, the NH groups are arranged in alternating order; in the protein I NMR structure (*7*), six of them are pointing outward, which could correspond to the amide protons seen to exchange with a decay time of 2 h, while 10 NH groups are pointing inward and participate to internal hydrogen bonds, most probably forming the β-core of amide protons we observed, which do not exchange within 5 days. Considering that in this protein part of the β-sheet structure is less shielded from the solvent by the rest of the molecule than in BPTI or protein K (*8*), one can conclude from our measurements that protein I β-sheet has probably limited flexibility.

The Reduction of the Bond 14−38 Has a Strong Destabilizing Effect on Protein I Structure. The major impact of reduction of the disulfide bond 14−38 was observed for protein I, the IR data revealing a significant broadening of the amide I′ band as well as a shift of the maximum toward lower wavenumbers (Figure 2b). Nevertheless, the absorption bands corresponding to α- and β-structures were still intense and not shifted, confirming the hypothesis that the structural changes, although more extensive in protein I than in the other two proteins, were limited to the modification site. As a result of the opening of a cleft in the structure, a fraction of 90% of the amide protons had completed exchange after only a few minutes of deuteration, and the stability of the β-sheet against exchange was dramatically lost, the core of amide protons exchanging 6−10-fold faster than in the corresponding BPTI species (Table 1 and Figure 3c).

The fluorescence emission of Trp35 in CM1,2-I was slightly redder (λ_{max} = 339.5 nm) than that in the native structure, indicative of a fluorophore only slightly more exposed to the solvent, and no change was observed in the calculated solvent accessibility. The fluorescence decay of Trp35 was not monoexponential any more and could be fitted by a sum of three exponential functions (Figure 5b), with a dominant lifetime of 4.4 ns accounting for 74% of the population, along with two shorter-lived components (Table 2). The existence of this long-lived component, after reduction of disulfide bond 14−38, corroborates the assumption of a strong quenching effect of the Trp fluorescence by this bond, in the native structure. The overall motion of the molecule accounted for 94% of the light depolarizing process, but a small proportion of a shorter correlation time could also be observed, confirming that some segmental motion had become possible to a small degree in the modified protein (Table 3). Interestingly, the measured hydrodynamic radius of CM1,2-I was not larger than that observed for the native molecule (Table 3).

In the modification site of protein I, two positive and one negative charges are located on the same loop, and the attractive effect of the blocking group on Cys38 with Arg13 and Lys17 could be counterbalanced by a repulsive effect with Asp10. This competition between different electrostatic interactions could explain the fact that the modification site was neither more expanded nor more compact upon reduction of 14−38 bond. Yet another alternative explanation could be that the hydrodynamic volume of CM1,2-I measured experimentally corresponds in fact to the average volume of a mixture of closed and open structures of CM1,2-I present in solution. Indeed, although no change in the volume of the molecule is apparently detectable after modification, the multiexponential intensity decay observed in CM1,2-I is an unambiguous indication that the flexibility of the loops has increased (Figure 5b). The presence of a second shorter correlation time of weak amplitude is also indicative that some wobbling of Trp35 could occur in CM1,2-I that was not possible in the native conformation (Figure 6b).

The angular range of Trp 35 motion in the two species can be estimated from the anisotropy amplitude β_2 of the overall rotation of the molecule, using a model of diffusion within a cone of semi angle ω (*34* and Table 3). The semi angles obtained were 0° for the native protein and ranged between 11° and 17° for CM1,2-I. In contrast, the NMR data reported that no increase in the mobility of Tyr35 could be observed in BPTI, upon reduction of the bond 14−38 (*10*); these are indications that the stronger impact observed on the rates of exchange of the core residues for CM1,2-I compared to CM1,2-BPTI could be linked to a larger opening of the cleft after modification, resulting in a higher accessibility of the protons to the solvent, rather than to less stable hydrogen bonding within the β-structure.

The Amide Proton Exchange in Toxins I and K Proceeds via a Breathing Protein Mechanism. When kinetics of exchange are investigated, the main question addressed is whether the mechanism of exchange of internal amide protons follows the "solvent penetration" model, achieved by diffusion inside the closed protein, or the two-state "breathing protein" model, which implies an equilibrium between closed and open forms of the molecule (*36*). All the results presented here are in favor of an exchange via the breathing model for the proteins K and I. The molecule of CM1,2-K is more closed and compact than the native form, and the faster rates of exchange observed after reduction of cystine 14−38 are incompatible with a penetration model. Likewise, very similar molecular volumes and accessibilities of Trp35 to acrylamide have been observed for CM1,2-I and native protein I (Table 3), and the increased mobility of Trp35 as well as the faster rates of exchange of internal residues after modification can only be explained if a mixture of open and closed forms exists in solution. This conclusion is further confirmed by the fluorescence decays data of CM1,2-I indicating the existence of two major conformers: the more populated one with a lifetime of 4.4 ns could correspond to a closed form, where the fluorophore has limited freedom of rotation, while the component of 1.4 ns could correspond to a more open form, where Trp35 has a higher motional freedom. A two-dimensional analysis of the polarized fluorescence decays supports this proposal. Using a model postulating any a priori association between lifetimes τ_i and correlation times θ_i (*37*), a clear association between the ∼1.4 ns lifetime and a nanosecond rotation (peak 2 of Figure 7) can be evidenced, the major long lifetime being associated with the Brownian rotational correlation time of ∼4 ns (peak 1); peak 3 of Figure 7 corresponds to a very fast Trp35 dynamics, specific of the shortest lifetime of the Figure 5b, but poorly weighted. The hydrodynamic volumes of these two forms would not differ enough for their motional correlation times to be resolved independently.

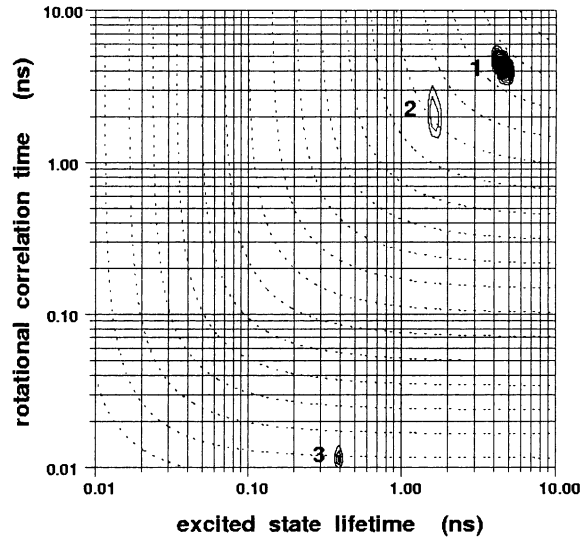

FIGURE 7: Two-dimensional $\Gamma(\tau,\theta)$ plot resulting from analysis by MEM of the CM1,2-I vertically and horizontally polarized fluorescence decays

$$I_{vv}(t) = 1/3\int_0^\infty\int_0^\infty \Gamma(\tau,\theta)e^{-t/\tau}(1 + 2Ae^{-t/\theta})\,d\tau\,d\theta$$

$$I_{vh}(t) = 1/3\int_0^\infty\int_0^\infty \Gamma(\tau,\theta)e^{-t/\tau}(1 - Ae^{-t/\theta})\,d\tau\,d\theta$$

with a fixed value of 0.25 for the intrinsic (or fundamental) anisotropy *A*.

CONCLUSIONS

In the present studies, we investigated the impact of local structural changes on the backbone flexibility of a folded conformation, by comparing three homologous proteins, BPTI, protein K, and protein I, using FTIR and time-resolved fluorescence spectroscopy approaches. The results obtained are in close agreement with the NMR data, when available, and have laid the foundations for a future structural analysis of the partially folded states that accumulate in the refolding of the three proteins and for which no structure is known. Moreover, this work shed a new light on the nature of the differences in thermal stability previously reported for these proteins, but never clearly elucidated (*6*, *9*).

In contrast with BPTI, where the elements of secondary structures, as well as the tertiary structure, are highly rigid, the protection of protein K against hydrogen/deuterium exchange seems to arise mainly from a very compact three-dimensional conformation as, internally, the molecule was shown to be 10-fold less protected than BPTI or protein I. The most probable destabilizing element was identified as Pro32, in the core of the β-sheet. Of the three homologues, protein I is known to be the least stable thermodynamically (*9*); yet the present investigations gave clear evidence that this lower stability arose mainly from the more expanded conformation of the molecule, as the secondary structure elements appeared to have limited flexibility, probably in order to maintain the three-dimensional, biologically active, structure of the less protected molecule.

Proteins with homologous amino acid sequences are always found to present similar folded conformations, and the interior residues that are important for the 3D-conformation are usually highly conserved (*30*, *38*, *39*). Drastic, naturally occurring substitutions, such as the introduction of a proline in the core of a β-sheet or the deletion of a strongly stabilizing salt bridge, are known to have substantial effects on the thermal stability of a molecule (*30*), and when they occur, they are often dictated by functional imperatives.

Although structurally homologous to the Kunitz-type protease inhibitors such as BPTI, protein I, and protein K have no inhibitory activity for proteases but are potent voltage-gated potassium channel blockers (*40*). Protein K was shown to specifically target Kv1.1 potassium channels (*1*), and residues Trp25 and Lys26 in the β-turn and Lys3 and Lys6 in the N-terminus were identified by site-directed mutagenesis as being functionally important (*41*). Interestingly, a different backbone conformation of the β-hairpin 18−35 has been observed by NMR (*6*) in protein K compared with BPTI, which was ascribed to the introduction of Pro32 in the β-sheet as well as to the necessity to accommodate Trp25 within the β-turn. These two substitutions could be linked, and the unusual introduction of Pro32 in the β-sheet during evolution could have been dictated by the necessity to generate a different backbone conformation at the β-turn, to fulfill the spatial requirements for Toxin K to bind to Kv1.1 potassium channels.

Protein I is less specific than Toxin K and was reported to block Kv1.1, Kv1.2, and Kv1.6 potassium channels expressed in *Xenopus* oocytes (*1*). Two regions of the molecule have been proposed as playing a role in Toxin I biological activity. One of them is the triad composed of Lys17/Tyr15/Trp35, located in the two loops region (*8*, *42*), and the higher flexibility observed in this region of protein I could be necessary for the protein to bind to potassium channels. The second site reported to be biologically important for Toxin I is Lys3 (BPTI numbering) located in the 3_{10}-helix, at the N-terminal end of the molecule (*43*), and it is not unconceivable that the different orientation of the N-terminal end reported for Toxin I might be necessary for this protein to bind to the Kv1.2 or Kv1.6 potassium channels.

REFERENCES

1. Robertson, B., Owen, D., Stow, J., Butler, C., and Newland, C. (1996) *FEBS Lett. 383*, 26−30.
2. Dufton, M. J. (1985) *Eur. J. Biochem. 153*, 647−654.
3. Laskowski, M., and Kato, I. (1980) *Annu. Rev. Biochem. 49*, 593−626.
4. Pardi, A., Wagner, G., and Wüthrich, K. (1983) *Eur. J. Biochem. 137*, 445−454.
5. Skarzynski, T. (1992) *J. Mol. Biol. 224*, 671−683.
6. Berndt, K. D., Güntert, P., and Wüthrich, K. (1993) *J. Mol. Biol. 234*, 735−750.
7. Foray, M. F., Lancelin, J. M., Hollecker, M., and Marion, D. (1993) *Eur. J. Biochem. 211*, 813−820.
8. Katoh, E., Nishio, H., Nishiuchi, Y., Kimura, T., Sakakibara, S., and Yamazaki, T. (2000) *Biopolymers 54*, 44−57.
9. Hollecker, M., and Creighton, T. E. (1983) *J. Mol. Biol. 168*, 409−437.
10. Wagner, G., Kalb, J., and Wüthrich, K. (1979) *Eur. J. Biochem. 95*, 249−253.
11. Hollecker, M., and Larcher, D. (1989) *Eur. J. Biochem. 179*, 87−94.
12. Richarz, R., Sehr, P., Wagner, G., and Wüthrich, K. (1979) *J. Mol. Biol. 130*, 19−30.
13. Wagner, G., and Wüthrich, K. (1982) *J. Mol. Biol. 160*, 343−361.
14. Fringeli, U. P., and Günthard, H. H. (1981) in *Membrane Spectroscopy* (Grell, E., Ed.) pp 270−332, Springer-Verlag, Berlin.
15. Goormaghtigh, E., Vigneron, L., Scarborough, G. A., and Ruysschaert, J. M. (1994) *J. Biol. Chem. 269*, 27409−27413.
16. De Jongh, H. H. J., Goormaghtigh, E., and Ruysschaert, J. M. (1997) *Biochemistry 36*, 13593−13602.

17. Vincent, M., Gallay, J., and Demchenko, A. P. (1995) *J. Phys. Chem. 99*, 14931−14941.
18. Brochon, J. C. (1994) *Methods Enzymol. 240*, 262−311.
19. Vincent, M., and Gallay, J. (1991) *Eur. Biophys. J. 20*, 183−191.
20. Sopkova, J., Vincent, M., Lewit-Bentley, A., and Gallay, J. (1999) *Biochemistry 38*, 5447−5458.
21. Li de La Sierra, I. M., Gallay, J., Vincent, M., Bertrand, T., Briozzo, P., Barzu, O., and Gilles, A. M. (2000) *Biochemistry 39* (*51*), 15870−15878.
22. Suzy, H., Timasheff, S. N., and Stevens, L. (1967) *J. Biol. Chem. 242*, 5460−5466.
23. Wagner, G. (1983) *Q. Rev. Biophys. 16*, 1−57.
24. Wagner, G., and Wüthrich, K. (1979) *J. Mol. Biol. 130*, 31−37.
25. Wagner, G., and Wüthrich, K. (1979) *J. Mol. Biol. 134*, 75−94.
26. Wagner, G., Stassinopoulou, C. I., and Wüthrich, K. (1984) *Eur. J. Biochem. 145*, 431−436.
27. Goossens, K., Smeller, L., Frank, J., and Heremans, K. (1996) *Eur. J. Biochem. 236*, 254−262.
28. Jackson, M., and Mantsch, H. H. (1995) *Crit. Rev. Biochem. Mol. Biol. 30* (*2*), 95−120.
29. Takeda, N., Nakano, K., Kato, M., and Taniguchi, Y. (1998) *Biospectroscopy 4*, 209−216.
30. Creighton, T. E. (1993) in *Proteins: Structures and Molecular Properties*, 2nd ed. (Creighton, T. E., Ed.) pp 188 and 287−308, W. H. Freeman and Company, New York.
31. Brown, L. R., De Marco, A., Richarz, R., Wagner, G., and Wüthrich, K. (1978) *Eur. J. Biochem. 88*, 87−95.
32. Chen, Y., and Barkley, M. D. (1998) *Biochemistry 37*, 9976−9982.
33. Lakowicz, J. R. (1999) in *Principles of Fluorescence Spectroscopy* 2nd ed., p 237, Kluwer Academic, Dordrecht, The Netherlands.
34. Eftink, M. R. (1991) *Methods Bioch. Anal. 35*, 127−205.
35. Eftink, M. R., and Ghiron, C. A. (1976) *Biochemistry 15*, 672−680.
36. Englander, S. W., Downer, N. W., and Teitelbaum, H. (1972) *Annu. Rev. Biochem. 41*, 903−924.
37. Rouviere, N., Vincent, M., Craescu, C., and Gallay, J. (1997) *Biochemistry 36, 7339−7352*.
38. Creighton, T. E. (1975) *Nature (London) 255*, 743−745.
39. Dufton, M. J. (1985) *Eur. J. Biochem. 153*, 647−654.
40. Harvey, A. L., and Anderson, A. J. (1991) in *Snake Toxins* (Harvey, A. L., Ed.), pp 131−164, Pergamon Press, New York.
41. Wang, F. C., Bell, N., Reid, P., Smith, L. A., McIntosh, P., Robertson, B., and Dolly, J. O. (1999) *Eur. J. Biochem. 263*, 222−229.
42. Hollecker, M., Marschall, D. L., and Harvey, A. (1993) *Br. J. Pharmacol. 110*, 790−794.
43. Harvey, A. L., Rowan, E. G., Vatanpour, H., Engström, A., Westerlund, B., and Karlsson, E. (1997) *Toxicon 35*, 1263−1273.

BI0204950